Pergamon

Int. J. Heat Mass Transfer. Vol. 41, No. 2, pp. 287–292, 1998

Printed in Great Britain
0017–9310/98 $19.00 + 0.00

PII: S0017–9310(97)00142–7

Velocity and temperature wall laws in a vertical concentric annular channel

J. A. ZARATE, M. CAPIZZANI and R. P. ROY†

Department of Mechanical and Aerospace Engineering, Arizona State University, Tempe, AZ 85287-6106, U.S.A.

(*Received* 25 *September* 1996 *and in final form* 14 *May* 1997)

Abstract— Logarithmic wall laws of mean axial velocity and temperature are obtained for the heated inner wall of a vertical concentric annular channel from measurements in turbulent liquid flow. The temperature wall law has limited generality because Prandtl number only in the range 7–8 is considered. When the influence of the buoyancy force as indicated by the parameter $Gr_q/Pr\,Re^4$ becomes large, the velocity and temperature data do not follow the respective wall laws. © 1997 Elsevier Science Ltd.

INTRODUCTION

We consider a vertical concentric annular channel whose inner wall is heated (axially uniform heat flux) and the outer wall insulated. Our objective is to obtain logarithmic wall laws of fluid mean axial velocity and temperature for the inner wall on the basis of measurements in heated turbulent flow. The inner wall law for mean axial velocity in isothermal flow has been found to depart noticeably from that for a flat plate and circular pipe [1–3]. This departure appeared to depend mainly on the ratio of the inner radius of the annulus to its outer radius. Patel [4] suggested that a possible reason for the departure is the convexity of the annulus inner wall. There the velocity wall law changes discernibly from the isothermal law upon introduction of heating is an issue in need of attention.

As for the fluid mean temperature, Johnk and Hanratty [5] proposed a wall law for turbulent flow in a vertical pipe at low wall heat fluxes. It has been suggested also that the additive constant in the logarithmic wall law for temperature in flat plate and pipe flows is a function of the fluid Prandtl number [6–8]. Polyakov [9] found that the friction factor, the Nusselt number, and the velocity and temperature wall laws for turbulent heated flow in a vertical circular pipe are modified significantly by the buoyancy forces in the flow field. He suggested two different effects of buoyancy: an external effect which acts on the mean field and a structural effect which affects the turbulent transport. Furber *et al.* [10] reported the heat transfer coefficient and the friction factor for turbulent forced convection heat transfer to helium and nitrogen gases in an annular channel. The friction factor was found to decrease as the ratio of the wall temperature to the fluid bulk temperature increased.

The Reynolds number range covered in our study is 22 800–40 200. The Grashof number, Gr, range is 1×10^7–4.2×10^7 and the range of Gr/Re^2 0.006–0.08. The measurements were made sufficiently downstream of the beginning of heated length such that the flow would be fully developed in the event of small fluid property variations.

EXPERIMENTAL APPARATUS

The experimental rig has been described previously [11]. Refrigerant 113 (R-113) was the working liquid. Its flow rate through the annular test section was measured by a turbine flow meter. Also monitored during the experiments were the liquid temperatures at the test section inlet and exit (by copper–constantan thermocouples) and the inlet and exit pressures (by Bourdon-tube pressure gauges).

The test section

A detailed description can be found in Velidandla *et al.* [3]. The concentric annular geometry is shown schematically in Fig. 1. The 3.66 m long channel was comprised of a 304 stainless steel inner tube (i.d. = 14.6 mm, o.d. = 15.8 mm) whose upper 2.75 m length could be resistively heated by direct current. The outer tube of the channel was of transparent pyrex glass (i.d. = 38.1 mm, o.d. = 47.0 mm), except for a 0.521 m long section where the velocity and temperature measurements were made. The outer tube of this measurement section was of optical quality quartz (i.d. = 37.9 mm, o.d. = 41.8 mm). The axial plane of measurement (m.p.) was 0.424 m ($\approx$19 hydraulic diameters) downstream of the measurement section entrance, this entrance being in turn 1.51 m downstream of the beginning of the channel heated length. The test section, except for a 15 cm length of the quartz measurement section, was insulated on the outside with 50 mm thick fiber glass wool. The 15 cm length was jacketed by an anodized aluminum box

† Author to whom correspondence should be addressed.

NOMENCLATURE

C, C_H	additive constant in the wall law for velocity, temperature
c_p	fluid specific heat
D_h	annulus hydraulic diameter, $2(R_2-R_1)$
f	friction factor
g	gravitational acceleration
Gr, Gr_q	Grashof numbers: $g\beta(T_{w_1}-T_b)D_h^3/\nu^2$, $g\beta D_h^4 q''_{w_1}/k\nu^2$
h	heat transfer coefficient
k	fluid thermal conductivity
Nu	Nusselt number, hD_h/k
p	thermodynamic pressure
p'	defined as $(p+\rho gz)$
Pr	Prandtl number
q''_{w_1}	inner wall heat flux
r	radial coordinate
R_0	radial location of zero axial shear stress
R_1, R_2	radius of inner wall, outer wall
Re	Reynolds number, U_bD_h/ν
T, T_{w_1}	mean local fluid temperature, mean inner wall temperature
T^+	dimensionless local fluid temperature, $(T_{w_1}-T)\rho c_p U_{\tau_1}/q''_{w_1}$
U, U_b, U_{τ_1}	local mean axial velocity, bulk velocity, inner wall friction velocity
U^+	dimensionless local axial velocity, U/U_{τ_1}
$\overline{uv}$	single-point cross-correlation between the liquid axial velocity and radial velocity fluctuations
y	coordinate normal to wall
y^+	nondimensional wall coordinate, yU_{τ_1}/υ
y_0^+	wall coordinate at zero axial shear stress location
z	axial coordinate.

Greek symbols

β	volumetric expansion coefficient, $-(1/\rho)(\partial\rho/\partial T)_p$
κ, κ_H	von Karman constant for velocity, temperature
ν	fluid kinematic viscosity
ρ	fluid density
τ_{w_1}, τ_{w_2}	axial shear stress at inner wall, outer wall.

Subscripts

in	inlet
m.p.	measurement plane
nb	buoyancy free
r	cross-sectional average value.

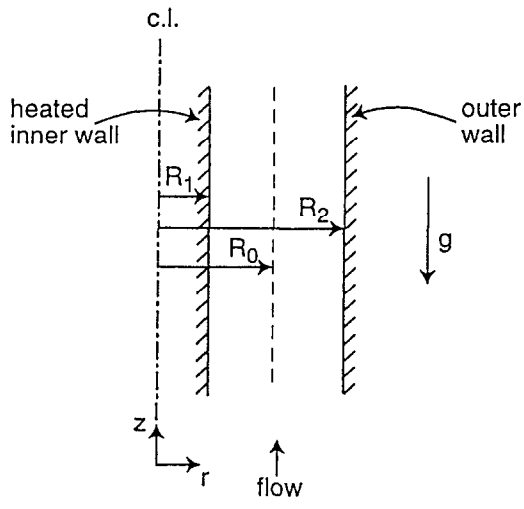

Fig. 1. The concentric annular channel.

with quartz windows and filled with liquid R-113 to facilitate laser Doppler velocimeter (LDV) measurements.

The heating power input to the test section was calculated as the product of the magnitude of direct current from a d.c. power supply (Rapid Technologies; 40 volts, 1500 amperes maximum) and the voltage difference across the heated tube. The input when divided by the outer surface area of the heater tube yielded the inner wall heat flux.

Velocity measurement instrumentation

This has been described by Velidandla *et al.* [3]. Briefly, it consisted of an LDV (TSI) featuring a 100 mW argon–ion laser and an 83 mm fiberoptic probe (250 mm nominal focal length) equipped with a backscatter light detector. The system also contained a retro-reflector module consisting of a reflecting prism and a focusing lens. White nylon particles of 3–7 μm size were used to seed the flow.

Temperature measurement instrumentation

The chromel–alumel microthermocouple which measured the mean liquid temperature distribution has been described by Beckman *et al.* [12]. The time constant of the microthermocouple in liquid R-113 flow at the experiment velocities is about 2 ms.

RESULTS AND DISCUSSION

Velocity field

Eight different experiments, Table 1, were analyzed. However, only experiments 3–8 were considered in

Table 1. The experiments considered

Exp.	T_{in}, °C	q''_{w_1}, W m^{-2}	$Pr_{m.p.}$	Re_{in}	$Gr_{q,m.p.} \times 10^{-9}$	$Gr_{m.p.} \times 10^{-7}$	$(Gr_q/PrRe^4)_{m.p.} \times 10^{10}$
1	42.7	9005	7.17	22825	3.7	2.3	17.86
2	42.7	15996	7.09	22890	6.9	4.2	30.80
3	30.3	8999	7.98	28450	2.6	1.3	4.78
4	30.3	16007	7.92	28350	4.8	2.3	8.49
5	42.7	9000	7.20	31500	3.7	1.7	4.97
6	42.7	16000	7.15	31200	6.5	3.0	8.80
7	31.2	9212	7.95	40175	2.7	1.0	1.25
8	31.2	15945	7.89	40175	4.9	1.7	2.20

obtaining the inner wall velocity law. The reason for this is stated later. In the logarithmic region ($40 \leqslant y^+ \leqslant y_0^+$), the mean axial velocity profile was to be represented by

$$U^+ = \frac{1}{\kappa}\ln y^+ + C. \tag{1}$$

To find κ and C, it was necessary to know U_{τ_1}, the friction velocity at the inner wall. It was determined as follows: the flow field can be subdivided into two radial regions delimited by the zero axial shear stress (turbulent plus viscous) location, R_0. This location was obtained from the heated flow $\overline{uv}$ measurements†, the uncertainty being $\pm 2\%$. Assuming fully developed condition, uniform pressure over the cross-section and that the buoyancy forces can be represented following the Boussinesq approximation, equations for the shear stress at the inner and outer walls were obtained by radially integrating the axial momentum equation over each region:

$$R_1\tau_{w_1} = \int_{R_1}^{R_0} \rho_r g\beta(T-T_r)r\,dr + \left(-\frac{1}{2}\frac{dp'}{dz}\right)(R_0^2 - R_1^2) \tag{2}$$

$$R_2\tau_{w_2} = \int_{R_0}^{R_2} \rho_r g\beta(T-T_r)r\,dr + \left(-\frac{1}{2}\frac{dp'}{dz}\right)(R_2^2 - R_0^2). \tag{3}$$

The two terms on the RHS of equations (2) and (3) are, respectively, the buoyancy force and the pressure force per unit length of the channel. The buoyancy term was evaluated by numerical integration using the measured mean liquid temperature profile, Velidandla *et al.* [3].

The friction factor is defined as:

$$f = -\frac{D_h}{2\rho U_b^2}\frac{dp'}{dz}. \tag{4}$$

Combining equations (2) and (4)

$$R_1\tau_{w_1} = \int_{R_1}^{R_0} \rho_r g\beta(T-T_r)r\,dr + \frac{(R_0^2 - R_1^2)}{(R_2 - R_1)}\frac{\rho_b U_b^2 f}{2}. \tag{5}$$

If R_0 and f are known in equation (5), then τ_{w_1} can be determined and U_{τ_1} evaluated. We calculated f from the Blasius equation

$$f = 0.079Re^{-0.25} \tag{6}$$

the liquid properties having been evaluated at the axially-local film temperature for the inner wall. Furthermore, in order to account for the effect of buoyancy, the friction factor was corrected whenever Gr_q was greater than $2\times 10^{-4} Pr\ Re^{2.75}$ as suggested by Polyakov [9]:

$$\frac{f}{f_{nb}}\left(1 - \sqrt{\frac{f}{f_{nb}}}\right) = 25\frac{Gr_q}{PrRe^{2.75}}. \tag{7}$$

Once U_{τ_1} was determined for each experiment, the measured mean axial velocity profiles ($40 \leqslant y^+ \leqslant y_0^+$) were plotted in wall coordinates, Fig. 2. A best fit of the data yielded the following relation:

$$U^+ = 2.5\ln y^+ + 5.7. \tag{8}$$

The uncertainty in $1/\kappa$, the coefficient of $\ln y^+$, is ± 0.05. The uncertainty in the additive constant is ± 0.4. This relation is shown in Fig. 2.

Also shown in Fig. 2 is our isothermal logarithmic wall law. To obtain this wall law, U_{τ_1} was calculated from equation (5), but without the buoyancy term, and equation (6). This isothermal wall law for velocity differs from the one reported in [3] because in the latter, U_{τ_1} was determined in a different manner: the mean axial velocity data was used to find the best estimate of the ratio U_{τ_1}/κ and then the optimum values of the pair (U_{τ_1}, κ) were determined by trial and error. This approach [3] may have introduced greater uncertainty in U_{τ_1}.

Figure 2 also contains the minimum and maximum values of y_0^+ among the eight experiments. A few points should be noted at this juncture. Firstly, our measurements did not extend into the laminar sublayer. This is because the LDV data rate dropped

† This is appropriate since the contribution of the viscous shear stress in this region is negligible.

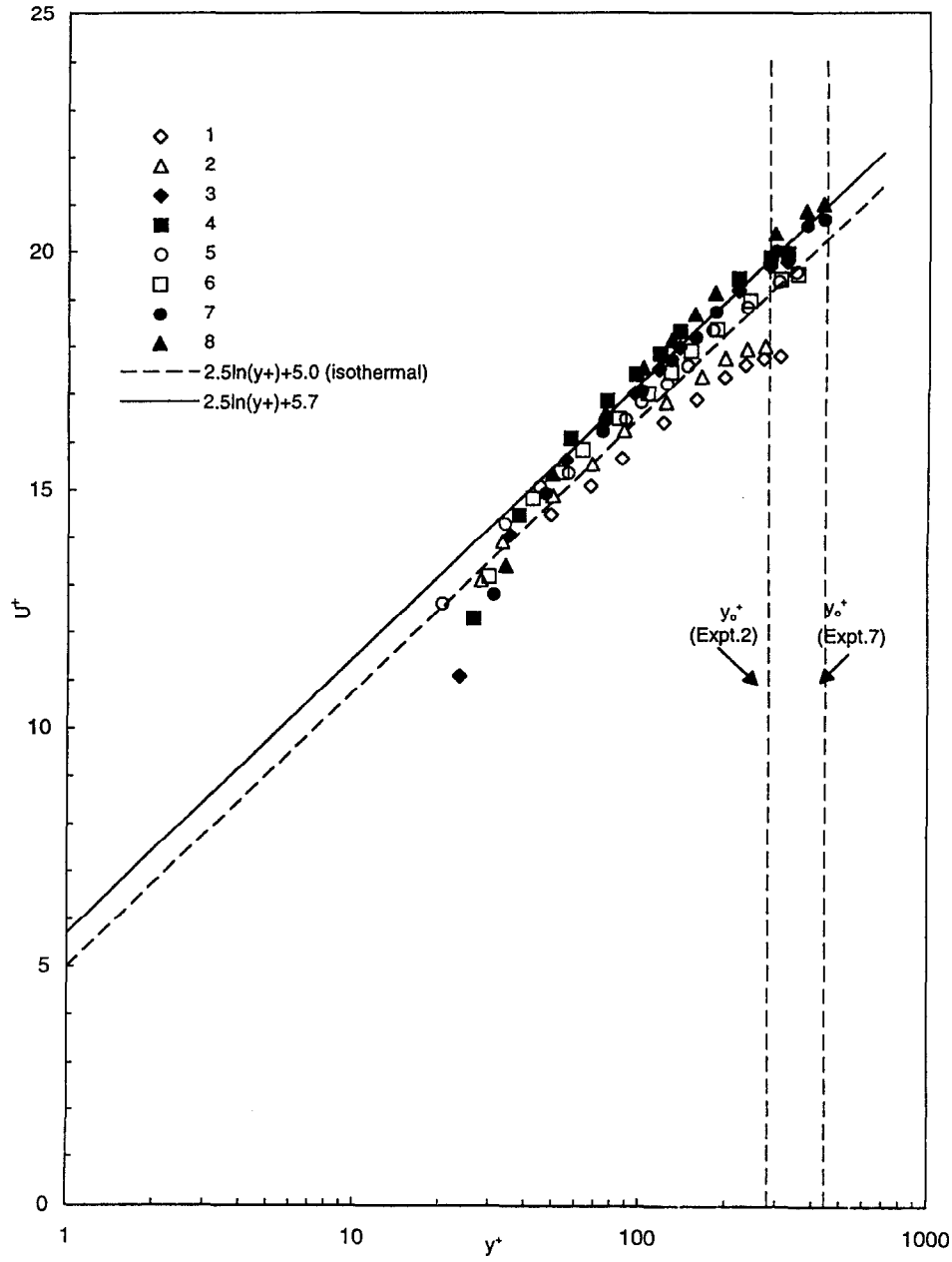

Fig. 2. Velocity law for inner wall.

significantly near the heated wall due to thermophoresis. Secondly, the logarithmic wall law for the heated inner wall, equation (8), differs only slightly from the isothermal law, the difference being in the value of the additive constant. Lastly, the $U^+ - y^+$ profiles of experiments 1 and 2 deviate markedly from those of experiments 3–8.

The change in the value of τ_{w_i} with increase in wall heat flux can be analyzed by equation (5). The second term on the RHS of equation (5) decreases as the wall heat input increases because R_0 and f decrease. On the other hand, the first term on the RHS (the buoyancy term) increases because $(T - T_r)$ increases. The net change in τ_{w_i} and hence, in U_{τ_i} depend on the relative contributions of the two terms. The only experiments where τ_{w_i} increased in comparison to the corresponding isothermal values are experiments 1 and 2.

The inner wall law is affected not only by the change in τ_{w_i}, but also by the modification of the mean axial velocity field that is induced by the heating. On one hand, the $U^+ - y^+$ profile moves down (in the $U^+ - y^+$ plot) as U_{τ_i} increases; on the other, the $U^+ - y^+$ profile moves up in much of the region between R_i and R_0 because the mean axial velocity increases. The net outcome of these two effects may be related to the nondimensional parameter $(Gr_q/PrRe^4)$, see Table 1, which represents the importance of buoyancy com-

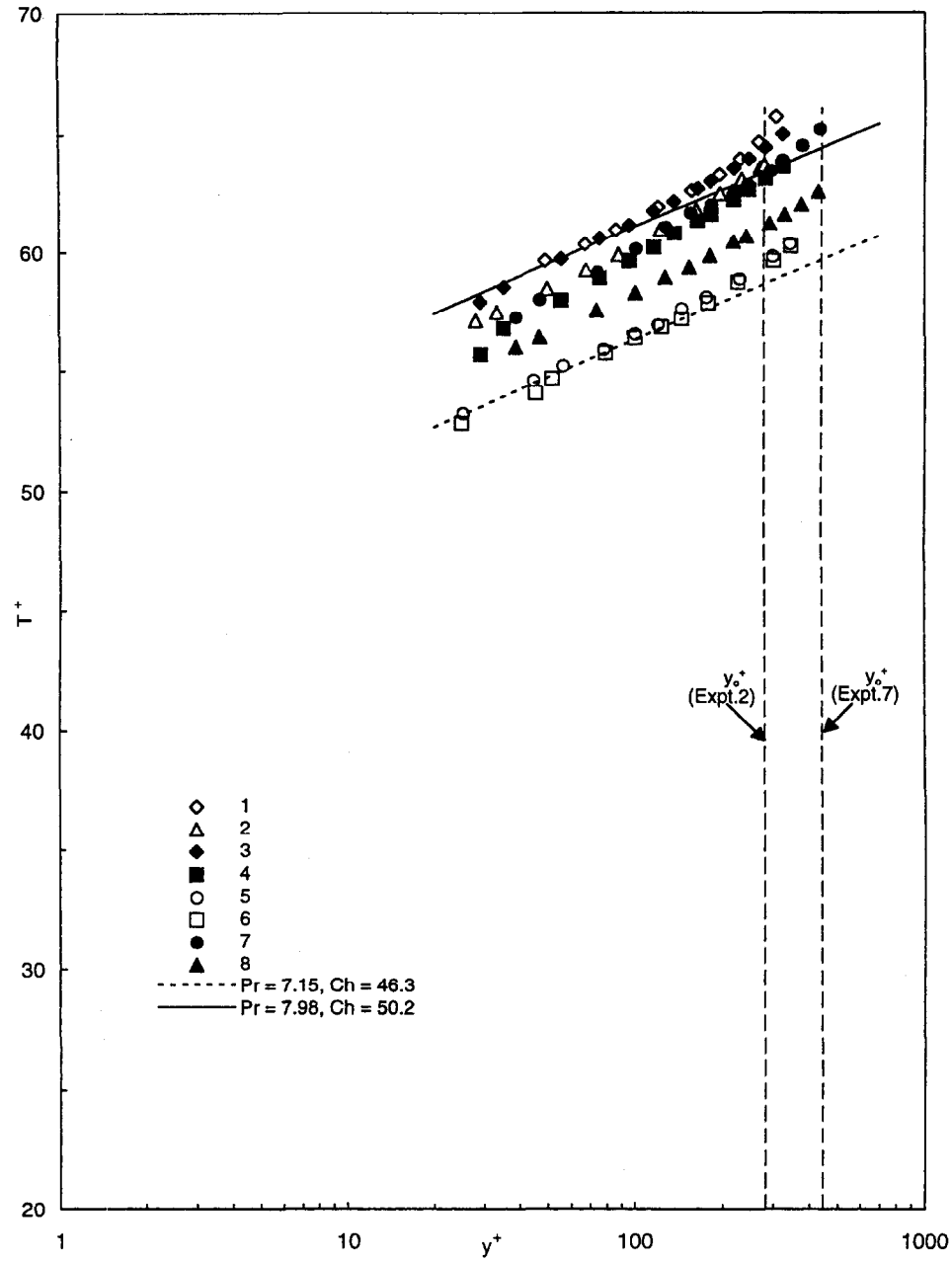

Fig. 3. Temperature law for inner wall.

pared to inertia. When this parameter is relatively small, as in experiments 3–8, the $U^+ - y^+$ profile moves up. When this parameter is large, as in experiments 1 and 2, the $U^+ - y^+$ profile shifts downward. Also, at sufficiently large values of $(Gr_q/PrRe^4)$ the $U^+ - \ln y^+$ profile no longer remains linear.

Temperature field

The eight experiments listed in Table 1 were analyzed and as in the case of the velocity only experiments 3–8 were considered to obtain the temperature wall law. Figure 3 shows plots of T^+ vs y^+ for all eight experiments and the maximum and minimum y_0^+.

It has been suggested that there exists a logarithmic region for the mean fluid temperature similar to that for the mean axial velocity:

$$T^+ = \frac{1}{\kappa_H} \ln y^+ + C_H. \tag{9}$$

The mean inner wall temperature is needed to calculate T^+. This was calculated from a correlation proposed by Hasan *et al.* [13] from wall and liquid temperature measurements in the same test section:

$$Nu = 0.0106 Re^{0.88} Pr^{0.4} \tag{10}$$

with the liquid properties evaluated at the local bulk temperature.

Table 2. Measurement uncertainties

	Uncertainty*
Reynolds number at test section inlet	±100
Wall heat flux	±100 W m^{-2}
Mean liquid temperature at test section inlet	±0.1°C
m.p. pressure/R-113 partial pressure at m.p. (sat. temp.)	±1 kPa (±0.2°C)
Local mean liquid temperature at m.p.	±0.2°C
Wall (heated) temperature at m.p.	±0.4°C

* The uncertainty estimates are for 95% confidence.

A best fit of the data for experiments 3–8 resulted in an average κ_H value of 0.44. As for C_H, it exhibited a dependence on the Prandtl number as has been suggested by Gowen and Smith [6] and Kader [8]. C_H could be represented by a modification of Kader's expression:

$$C_H(Pr) = 2.25\ln(Pr) + [3.8Pr^{1/3} - 0.85]^2. \quad (11)$$

The uncertainty for κ_H was ±0.02 while for C_H ±1.0.

Figure 3 also contains plots of our temperature logarithmic wall law corresponding to the highest and lowest Prandtl number values among the six experiments (experiments 3 and 6, respectively). The experimental data and the suggested wall law agree reasonably well. Experiments 1 and 2 again deserve special attention because they do not comply with the Prandtl number trend denoted by equation (11) although the slope of the $T^+ - y^+$ profile remains similar to that of experiments 3–8. The upward shift of the $T^+ - y^+$ profile in the cases of experiments 1 and 2 can be explained in a manner similar to that for the velocity. Since T^+ is proportional to U_{τ_1}, a high friction velocity results in high T^+ values.

The profiles for all eight experiments also display a behavior similar to that of turbulent heated flow in a vertical pipe reported by Polyakov [9]. He found that for large buoyancy effects the $T^+ - y^+$ profile departs monotonically from the logarithmic wall law as y^+ increases. The higher the value of $Gr_q/PrRe^4$, the lower the y^+ value where this departure begins.

CONCLUDING REMARKS

Logarithmic velocity and temperature laws for the heated inner wall in turbulent liquid flow through a vertical concentric annular channel are proposed. The temperature wall law has limited generality because Prandtl number only in the range 7–8 is considered. The laws differ slightly from those for flow over a flat plate and through a circular pipe. The contribution of the buoyancy force was included and the Blasius relation for friction factor was used to evaluate the shear stress at the inner wall. The use of Blasius friction factor is different from the approach taken by Velidandla *et al.* [3] and the velocity wall obtained is different as a result. A modification of Kader's expression [8] for the additive constant in the temperature law, C_H, is suggested.

When the influence of the buoyancy force becomes large, the velocity and temperature data do not follow the respective wall laws. The nondimensional parameter $Gr_q/PrRe^4$ appears to be a good indicator of the buoyancy effect relative to that of inertia. Finally, the average turbulent Prandtl number computed from the ratio κ/κ_H is approximately 0.9.

Acknowledgements—This research was supported by National Science Foundation, Thermal System Program, Division of Chemical and Thermal Systems, under grant no. CTS-9411898. Funding from Electric Power Research Institute and Electricité de France is also gratefully acknowledged. Funding for J. A. Zarate was provided by Consejo Nacional de Ciencia y Tecnologia, Mexico.

REFERENCES

1. Brighton, J. A. and Jones, J. B., Fully developed turbulent flow in annuli. *Journal of Basic Engineering*, 1964, **86,** 835–844.
2. Lawn, C. J. and Elliot, C. J., Fully developed turbulent flow through concentric annuli. *Journal of Mechanical Engineering Science*, 1972, **14,** 195–204.
3. Velidandla, V., Putta, S. and Roy, R. P., Turbulent velocity field in isothermal and heated liquid flow through a vertical annular channel. *International Journal of Heat and Mass Transfer*, 1996, **39**(16), 3333–3346.
4. Patel, V. C., A unified view of the law of the wall using mixing-length theory. *Aeronautics Quarterly*, 1973, **24,** 55–70.
5. Johnk, R. E. and Hanratty, T. J., Temperature profiles for turbulent flow of air in a pipe—I. *Chemical Engineering Science*, 1962, **17,** 867–879.
6. Gowen, R. A. and Smith, J. W., The effect of the Prandtl number on temperature profiles for heat transfer in turbulent pipe flow. *Chemical Engineering Science*, 1967, **22,** 1701–1711.
7. Kader, B. A. and Yaglom, A. M., Heat and mass transfer laws for fully turbulent wall flows. *International Journal of Heat and Mass Transfer*, 1972, **15,** 2329–2351.
8. Kader, B. A., Temperature and concentration profiles in fully turbulent boundary layers. *International Journal of Heat and Mass Transfer*, 1981, **24,** 1541–1544.
9. Polyakov, A. F., Transient effects due to thermogravity in turbulence and heat transfer. *Heat Transfer—Soviet Research*, 1973, **11**(1), 90–98.
10. Furber, B. N., Appleby, G. G. and Facer, R. I., Forced convection heat transfer in an annulus. *Proceedings of the Fifth International Heat Transfer Conference*, 1974, **2,** 155–159.
11. Jain, P. K. and Roy, R. P., Stochastic characteristics of vapor fraction and wall pressure fluctuation in boiling flow. *International Journal of Multiphase Flow*, 1983, **9,** 463–481.
12. Beckman, P., Roy, R. P., Velidandla, V. and Capizzani, M., An improved fast-response microthermocouple. *Review of Scientific Instruments*, 1995, **66,** 4731–4733.
13. Hasan, A., Roy, R. P. and Kalra, S. P., Heat transfer measurements in turbulent liquid flow through a vertical annular channel. *ASME Journal of Heat Transfer*, 1990, **112,** 247–250.